Spin transport properties in double quantum rings connected in series*

Du Jian(杜坚)[1,†], Wang Suxin(王素新)[1], and Pan Jianghong(潘江洪)[2]

[1]Department of Physics, Hebei Normal College for Nationalities, Chengde 067000, China
[2]College of Physics and Technology, Guangxi Normal University, Guilin 541004, China

Abstract: A new model of metal/semiconductor/metal double-quantum-ring connected in series is proposed and the transport properties in this model are theoretically studied. The results imply that the transmission coefficient shows periodic variations with increasing semiconductor ring size. The effects of the magnetic field and Rashba spin-orbit interaction on the transmission coefficient for two kinds of spin state electrons are different. The number of the transmission coefficient peaks is related to the length ratio between the upper arm and the half circumference of the ring. In addition, the transmission coefficient shows oscillation behavior with enhanced external magnetic field, and the corresponding average value is related to the two leads' relative position.

Key words: transmission coefficient; double quantum rings; Rashba spin-orbit interaction
DOI: 10.1088/1674-4926/32/2/022001 **PACC:** 7340S; 7170C; 7335A

1. Introduction

With the development of spintronics, the spin transport properties of quantum rings have been extensively studied[1−6]. Recently, the remarkable discovery of the effect of the geometric phase has attracted considerable interest. Berry first discovered that there exists a geometric phase in adiabatic cycliaction's Hamilton system[7]. This finding provides a new method to study quantum structures. One can obtain an AB phase by changing the surrounding magnetic flux. The Berry phase can be interpreted as a holonomy associated with the parallel transport around a circuit in parameter space. Now, the relation between the Berry phase and quantum transport has been demonstrated. The persistent currents from the Berry phase in textured mesoscopic rings have been studied by Loss, Goldbart, and Balatsky[8]. There have been many studies on single ring, coupled ring, and connected ring structures[9−12]. In addition, the quantum transport properties of semiconductor ring structures with spin-orbit interaction (SOI) have attracted much attention[13−15].

In this paper, we propose a new model, which is a metal/semiconductor/metal quantum double-ring connected in series with two metal leads disposed symmetrically. The transmission coefficient properties in the model are investigated in the presence of Rashba spin-orbit interaction (RSOI) and magnetic flux. Our results further confirm that AB magnetic flux and Rashba spin-orbit interaction have important effects on the transmission coefficient.

2. Model and formula

The model studied in this paper is a metal/semiconductor/metal double-quantum-ring connected in series, as depicted in Fig. 1. The radius of the two rings is the same. In the double-ring, an asymmetric quantum well confining electrons in the z-axis direction gives rise to the Rashba spin-orbit interaction in the semiconductor region. It is assumed that the ring is sufficiently narrow. The Hamiltonian for Rashba spin-orbit interaction is

$$\hat{H}_{\mathrm{SO}} = \frac{\alpha}{\hbar}\left(\hat{\boldsymbol{\sigma}} \times \hat{\boldsymbol{p}}\right)_k . \tag{1}$$

Here, $\hat{\boldsymbol{\sigma}} = (\sigma_x, \sigma_y, \sigma_z)$ are Pauli spin matrices. The total Hamiltonian of a moving electron in the presence of a Rashba spin-orbit interaction can be found in Ref. [13]. Because the transverse width of the arm in the ring is narrow enough, and only the lower energy band is occupied at low temperature, the transverse motion of electron can be neglected. The quan-

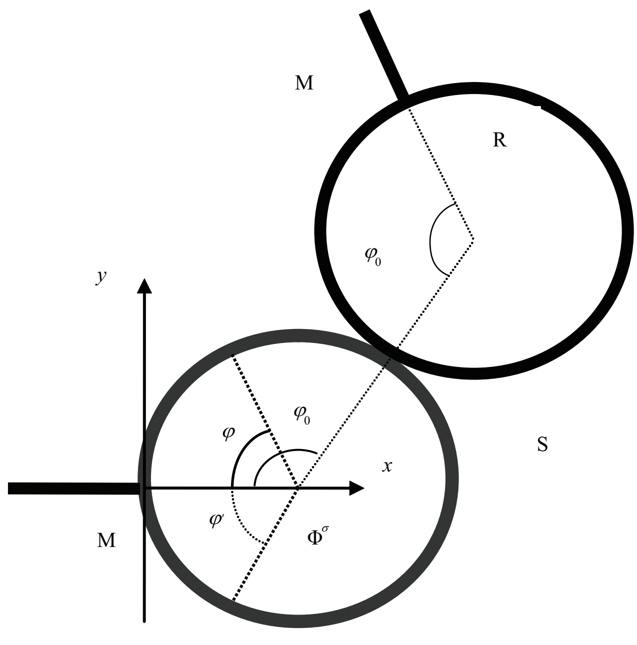

Fig. 1. Schematic diagram of double rings connected in series symmetrically coupled to two metal leads. The relative position of the two leads is described by angle φ_0.

* Project supported by the Natural Foundation of the Bureau of Education of Hebei Province, China (No. Z2008103).
† Corresponding author. Email: 808dujian@163.com

Received 6 August 2009, revised manuscript received 13 October 2010

tum ring is a strict one-dimensional (1D) ring, and completely meets the 1D waveguide theory. The total Hamiltonian[14] with AB magnetic flux can be written as

$$\hat{H}_{\rm s}=\frac{2m_{\rm s}^{*}R^{2}}{\hbar^{2}}\hat{H}_{\rm 1D}=\left(-{\rm i}\frac{\partial}{\partial\varphi}+\frac{\beta}{2}\sigma_{\gamma}-\frac{\Phi_{\rm AB}}{\phi_{0}}\right)^{2},\quad(2)$$

where $m_{\rm s}$* is the effective mass of the carrier, $\beta=2\alpha m_{\rm s}^{*}/\hbar^{2}$, $\sigma_{\gamma}=\cos\varphi\sigma_{x}+\sin\varphi\sigma_{y}$, $\Phi_{\rm AB}$ is the AB magnetic flux and $\phi_{0}=hc/e$ is quantum flux. The parameter α represents the average electric field along k direction and is assumed to be a tunable quantity. For an InGaAs-based quantum ring, α can be controlled by a gate voltage with typical values in the range $(0.5-2.0)\times10^{-11}$. According to Ref. [15], the energy eigenvalue in AB ring is

$$E_{\rm n}^{\sigma}=(n-\Phi_{\rm AC}/2\pi-\Phi_{\rm AB}/2\pi)^{2}.\quad(3)$$

Here, $\sigma=\pm1$, $\Phi_{\rm AC}^{\sigma}=-\pi\left(1-\sigma\sqrt{\beta^{2}+1}\right)$ is the so-called Aharonov–Casher (AC) phase. At fixed energy, the dispersion relation yields the quantum numbers $n_{\lambda}^{\sigma}(E)=\lambda\sqrt{E}+\Phi^{\sigma}/2\pi=\lambda kR+\Phi^{\sigma}/2\pi$, where $\Phi^{\sigma}=\Phi_{\rm AC}^{\sigma}+\Phi_{\rm AB}$ is the total magnetic flux. The wave functions can be formulated as

$$\Psi_{\sigma}^{\rm r}={\rm e}^{{\rm i}k_{\rm M}x}+r_{\sigma}{\rm e}^{-{\rm i}k_{\rm M}x},\quad(4)$$

$$\Psi_{\sigma}^{\rm t}=t_{\sigma}{\rm e}^{{\rm i}k_{\rm M}x},\quad(5)$$

$$\Psi_{{\rm LA},\sigma}^{\rm s}(\varphi)=\sum_{\sigma=\pm,\lambda=\pm}c_{{\rm LA},\sigma}^{\lambda}{\rm e}^{{\rm i}n_{\lambda}^{\varphi}\varphi}\chi^{\sigma}(\varphi),\quad(6)$$

$$\Psi_{{\rm LB},\sigma}^{\rm s}(\varphi')=\sum_{\sigma=\pm,\lambda=\pm}c_{{\rm LB},\sigma}^{\lambda}{\rm e}^{-{\rm i}n_{\lambda}^{\sigma}\varphi'}\chi^{\sigma}(\varphi'),\quad(7)$$

$$\Psi_{{\rm RA},\sigma}^{\rm s}(\varphi)=\sum_{\sigma=\pm,\lambda=\pm}c_{{\rm RA},\sigma}^{\lambda}{\rm e}^{{\rm i}n_{\lambda}^{\varphi}\varphi}\chi^{\sigma}(\varphi),\quad(8)$$

$$\Psi_{{\rm RB},\sigma}^{s}(\varphi')=\sum_{\sigma=\pm,\lambda=\pm}c_{{\rm RB},\sigma}^{\lambda}{\rm e}^{-{\rm i}n_{\lambda}^{\sigma}\varphi'}\chi^{\sigma}(\varphi'),\quad(9)$$

where $\chi^{\uparrow}(\varphi)=\frac{1}{2\sqrt{\pi}}\begin{pmatrix}\cos\vartheta/2\\ {\rm e}^{{\rm i}\varphi}\sin\vartheta/2\end{pmatrix}$, $\chi^{\downarrow}(\varphi)=\frac{1}{2\sqrt{\pi}}\begin{pmatrix}\sin\vartheta/2\\ {\rm e}^{{\rm i}\varphi}\cos\vartheta/2\end{pmatrix}$, $k_{\rm M}$ is the Fermi wave vector for metal, r and t denote the left and the right metal lead, L and R denote the left and the right quantum ring, and A and B denote the upper and lower arm in the identical ring, respectively.

Based on the practical current conservation principle and considering the influence of the spin rotation at the junction, the current density becomes

$$J^{\sigma}={\rm Re}\left[(\Psi^{\sigma}\chi^{\sigma})^{+}\left(-{\rm i}\frac{\partial}{\partial\varphi}+\frac{\beta}{2\sigma_{\gamma}}-\frac{\Phi_{\rm AB}}{\phi_{0}}\right)(\Psi^{\sigma}\chi^{\sigma})\right].\quad(10)$$

The wave vectors for the spin-up and spin-down electrons in the semiconductor region are $k_{+}^{\sigma}=k+\Phi^{\sigma}/2\pi R$ and $k_{-}^{\sigma}=k-\Phi^{\sigma}/2\pi R$, respectively. In the ring, $\varphi'=-\varphi$. When an electron moves along the upper arm in the clockwise direction from the input intersection at $\varphi=0$ (see Fig. 1), it acquires a phase $\Phi^{\sigma}/2$ at the output intersection $\varphi=\pi$, whereas the electron acquires a phase $-\Phi^{\sigma}/2$ in the counterclockwise direction along the other arm when moving from $\varphi'=0$ to $\varphi'=\pi$. When $\varphi_{0}=\pi$, taking into consideration the wave function of each segment and the boundary conditions, we obtain

$$1+r_{\sigma}=c_{{\rm LA}\sigma}^{+}+c_{{\rm LA}\sigma}^{-}{\rm e}^{-{\rm i}\Phi^{\sigma}/2}=c_{{\rm LB}\sigma}^{+}+c_{{\rm LB}\sigma}^{-}{\rm e}^{{\rm i}\Phi^{\sigma}/2},\quad(11)$$

$$\begin{aligned}t_{\sigma}{\rm e}^{{\rm i}k_{\rm M}\phi/2k}&=c_{{\rm RA}\sigma}^{+}{\rm e}^{{\rm i}(\phi+\Phi^{\sigma})/2}+c_{{\rm RA}\sigma}^{-}{\rm e}^{-{\rm i}\phi/2}\\&=c_{{\rm RB}\sigma}^{+}{\rm e}^{{\rm i}(\phi-\Phi^{\sigma})/2}+c_{{\rm RB}\sigma}^{-}{\rm e}^{-{\rm i}\phi/2},\end{aligned}\quad(12)$$

$$\begin{aligned}&c_{{\rm LA}\sigma}^{+}{\rm e}^{{\rm i}(\phi+\Phi^{\sigma})/2}+c_{{\rm LA}\sigma}^{-}{\rm e}^{-{\rm i}\phi/2}\\&=c_{{\rm LB}\sigma}^{+}{\rm e}^{-{\rm i}(\phi-\Phi^{\sigma})/2}+c_{{\rm LB}\sigma}^{-}{\rm e}^{-{\rm i}\phi/2}\\&=c_{{\rm RA}\sigma}^{+}+c_{{\rm RA}\sigma}^{-}{\rm e}^{-{\rm i}(\phi+\Phi^{\sigma})/2}\\&=c_{{\rm RB}\sigma}^{+}+c_{{\rm BR}\sigma}^{-}{\rm e}^{-{\rm i}(\phi-\Phi^{\sigma})/2},\end{aligned}\quad(13)$$

$$k_{\rm M}(1-r_{\sigma})=k\left(c_{{\rm LA}\sigma}^{+}-c_{{\rm LA}\sigma}^{-}{\rm e}^{-{\rm i}\Phi^{\sigma}/2}+c_{{\rm LB}\sigma}^{+}-c_{{\rm LB}\sigma}^{-}{\rm e}^{{\rm i}\Phi^{\sigma}/2}\right),\quad(14)$$

$$\begin{aligned}k_{\rm M}t_{\sigma}{\rm e}^{{\rm i}k_{\rm M}\phi/2k}&=k[c_{{\rm RA}\sigma}^{+}{\rm e}^{{\rm i}(\phi+\Phi^{\sigma})/2}-c_{{\rm RA}\sigma}^{-}{\rm e}^{-{\rm i}\phi/2}\\&\quad+c_{{\rm RB}\sigma}^{+}{\rm e}^{{\rm i}(\phi-\Phi^{\sigma})/2}-c_{{\rm RB}\sigma}^{-}{\rm e}^{-{\rm i}\phi/2}],\end{aligned}\quad(15)$$

$$\begin{aligned}&c_{{\rm LA}\sigma}^{+}{\rm e}^{{\rm i}(\phi+\Phi^{\sigma})/2}-c_{{\rm LA}\sigma}^{-}{\rm e}^{-{\rm i}\phi/2}+c_{{\rm LB}\sigma}^{+}{\rm e}^{-i(\phi-\Phi^{\sigma})/2}-c_{{\rm LB}\sigma}^{-}{\rm e}^{-{\rm i}\phi/2}\\&=c_{{\rm RA}\sigma}^{+}-c_{{\rm RA}\sigma}^{-}e^{-{\rm i}(\phi+\Phi^{\sigma})/2}+c_{{\rm RB}\sigma}^{+}-c_{{\rm BR}\sigma}^{-}e^{-{\rm i}(\phi-\Phi^{\sigma})/2},\end{aligned}\quad(16)$$

where $\phi=2\pi kR=2kL$. ϕ and kL are both physical quantities describing the quantum ring's size on account of $L=\pi R=\phi/2k$. Once t_{σ} is obtained, the transmission coefficient T^{σ} can be acquired from $T^{\sigma}=\frac{k_{\rm M}^{\rm R}}{k_{\rm M}^{\rm L}}|t_{\sigma}|^{2}$, and the average transmission coefficient can be defined as $\overline{T}^{\sigma}=\frac{1}{6\pi}\int_{0}^{6\pi}T^{\sigma}(kL)\,{\rm d}(kL)$.

3. Results and analysis

As shown in Fig. 2, we consider the case where electron transports through the metal/semiconductor/metal quantum rings connected in series. Firstly, we present the properties of the transmission coefficient as functions of kL/π with $\Phi^{\sigma}=0$ for different angles. Here, we can see that the transmission coefficient shows periodic equal amplitude oscillation with increasing semiconductor ring size. The phenomenon is induced by the quantum rings' size effects. Secondly, the whole vibration curves for spin-up electrons coincide closely with the spin-down electrons. It is well known that there will be no spin energy splitting phenomenon in the non-ferromagnetic terminal when $\Phi^{\sigma}=0$. So we can deduce that the circumstances for the two kinds of spin state tunneling electrons are completely same. That is the reason why they have the identical variation characteristics. Finally, the average transmission coefficient reaches a maximum for $\varphi_{0}=\pi$, as shown in Fig. 2(a). The result indicates that the average transmission coefficients for unequal arm rings are smaller than those for equal ones. So we conclude that the average hindrance to tunneling electrons in the unequal arm rings is stronger than that in equal arm rings.

In order to further understand the transmission properties of electrons in the presence of Rashba spin-orbit interaction, we assume $\beta=1.2$ and $\Phi_{\rm AB}=0$. The calculated results are plotted in Fig. 3. It is seen that the transmission coefficient curves

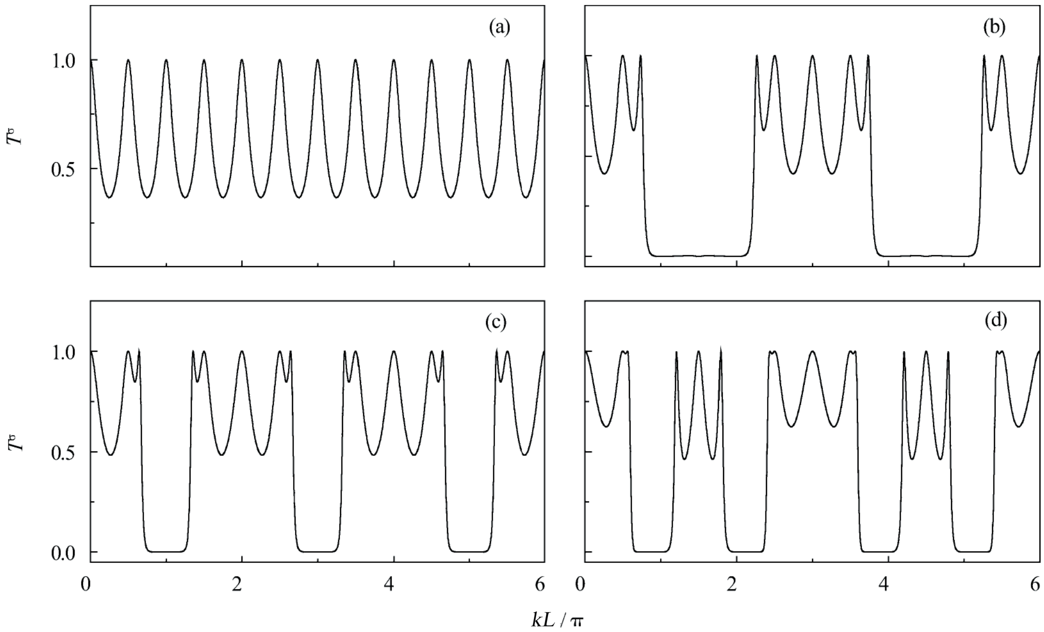

Fig. 2. Transmission coefficient as functions of kL/π with $\Phi^{\sigma} = 0$. φ_0 is set to be (a) $\varphi_0 = \pi$, (b) $\varphi_0 = 2\pi/3$, (c) $\varphi_0 = \pi/2$ and (d) $\varphi_0 = \pi/3$, respectively. The solid lines correspond to $T^{\uparrow}$ and the dotted lines correspond to $T^{\downarrow}$.

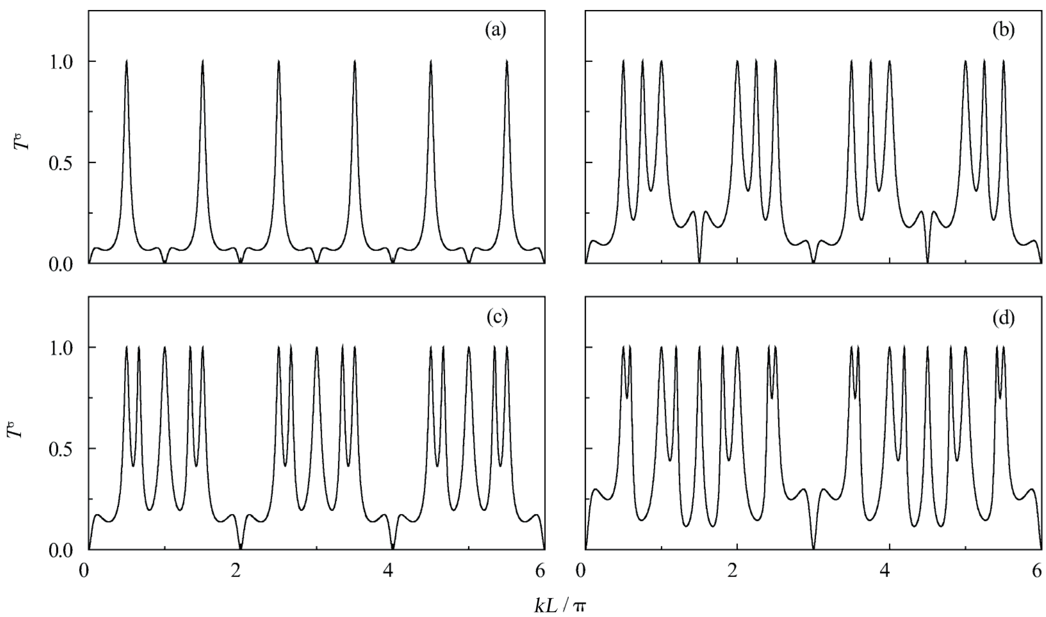

Fig. 3. Transmission coefficient as functions of kL/π with $\Phi_{\mathrm{AB}} = 0$ and $\beta = 1.2$. φ_0 is set to be (a) $\varphi_0 = \pi$, (b) $\varphi_0 = 2\pi/3$, (c) $\varphi_0 = \pi/2$ and (d) $\varphi_0 = \pi/3$. The solid lines correspond to $T^{\uparrow}$ and the dotted lines correspond to $T^{\downarrow}$.

show a remarkable variation compared with Fig. 2. This means that the Rashba spin-orbit interaction has an important influence on the transmission properties. Comparing the small chart (a) with the other small charts in Fig. 3, we can see that as the angle φ_0 decreases from $\varphi_0 = \pi$ to $\varphi_0 = 2\pi/3, \varphi_0 = \pi/2$ and $\varphi_0 = \pi/3$, the number of the main formants changes from 6 to 4, 3 and 2, respectively. This implies that there may be a certain connection between the number of the main formants and the two leads' relative positions. We define the ratio $\frac{L_{\mathrm{A}}}{\pi R} = \frac{N_{\mathrm{u}}}{N_{\mathrm{d}}}$, where L_{A} is the length of upper arm. Then corresponding to Figs. 3(a), 3(b), 3(c) and 3(d), the ratio will be $\frac{1}{1}$, $\frac{2}{3}$, $\frac{1}{2}$ and $\frac{1}{3}$, respectively. From Fig. 3(a), we can see the number of the main formants n_0 in the equal arm rings is 6, then we can obtain $\frac{3}{3} \times n_0 = 6$, $\frac{2}{3} \times n_0 = 4$, $\frac{1}{2} \times n_0 = 3$, $\frac{1}{3} \times n_0 = 2$ from $\frac{L_{\mathrm{A}}}{\pi R}\, n_0 = \frac{N_{\mathrm{u}}}{N_{\mathrm{d}}} n_0$ for φ_0 is π, $2\pi/3$, $\pi/2$ and $\pi/3$, respectively. So the number of the main formants for different angle φ_0 can be written as

$$n_{\mathrm{x}} = \frac{N_{\mathrm{u}}}{N_{\mathrm{d}}} n_0. \tag{17}$$

Here, n_{x} is the number of the main formants for different angle φ_0. This conclusion is valid only for a total magnetic flux is non-zero.

Additionally, in Fig. 4, we show the transmission coeffi-

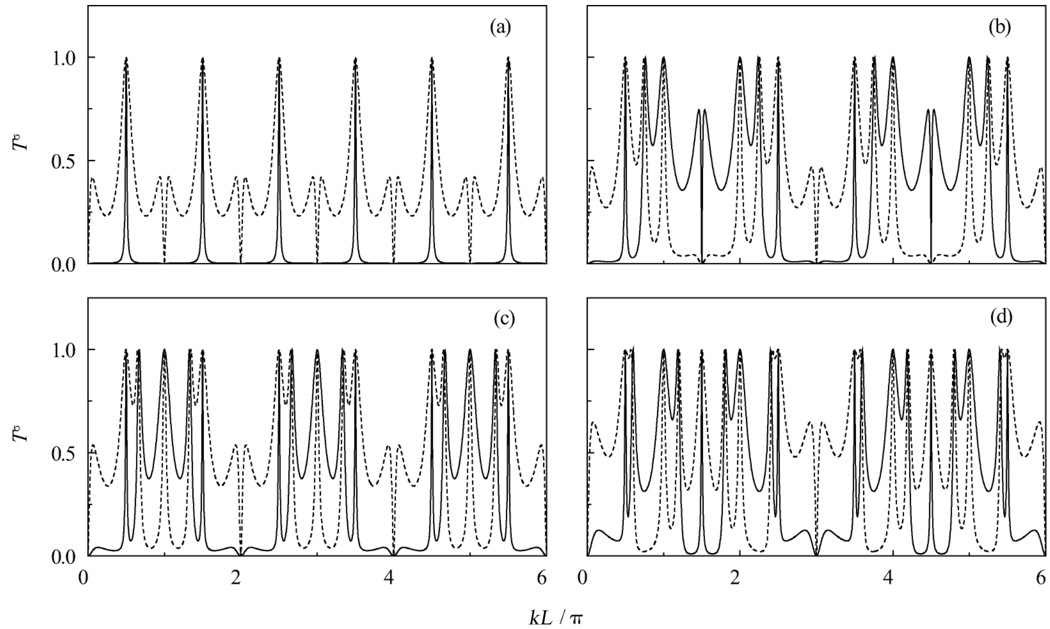

Fig. 4. Transmission coefficient as functions of kL/π under the condition of $\beta = 1.2$ and $\Phi_{\rm AB} = 0.24\pi$ for (a) $\varphi_0 = \pi$, (b) $\varphi_0 = 2\pi/3$, (c) $\varphi_0 = \pi/2$ and (d) $\varphi_0 = \pi/3$. The solid lines correspond to $T^\uparrow$ and the dotted lines correspond to $T^\downarrow$.

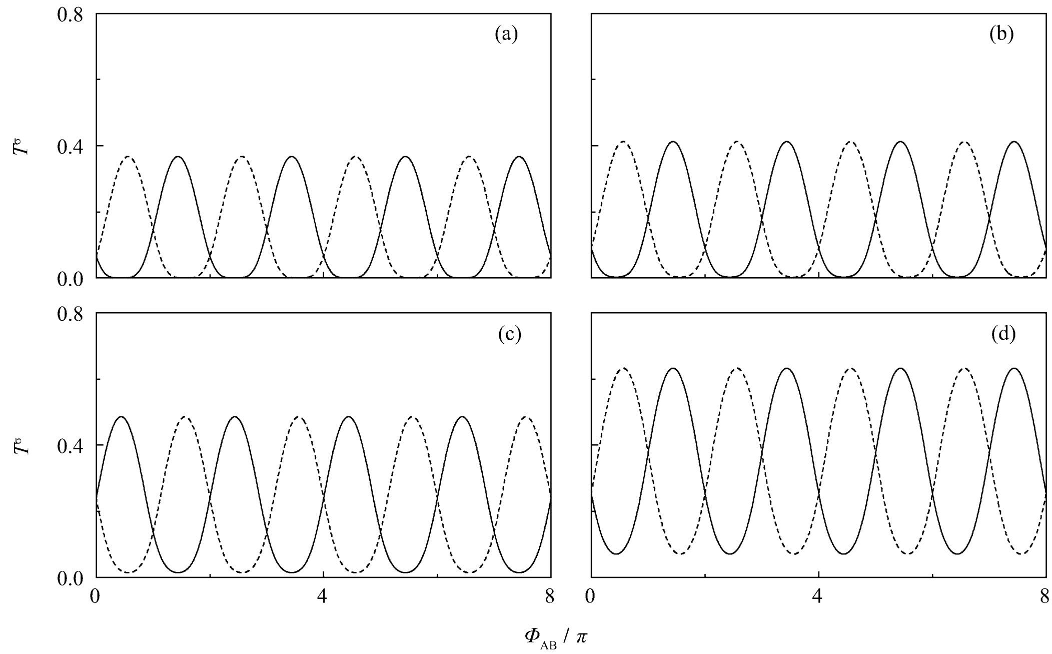

Fig. 5. Transmission coefficient as functions of the AB flux with $\beta = 1.2$ and $kL = 5.5\pi$ for (a) $\varphi_0 = \pi$, (b) $\varphi_0 = 2\pi/3$, (c) $\varphi_0 = \pi/2$ and (d) $\varphi_0 = \pi/3$, respectivily, where the solid lines correspond to $T^\uparrow$ and the dotted lines correspond to $T^\downarrow$.

cient as a function of kL/π in the presence of RSOI and AB magnetic flux. Here, we can obviously see that the curves of spin-up electrons are separated from that of spin-down electrons. Because the direction of the magnetic field is either parallel or anti-parallel to the spin orientation, the AB flux has different effects on the spin-up and spin-down electrons. To our excitement, we can see that the rule $n_{\rm x} = \frac{N_{\rm u}}{N_{\rm d}} n_0$ is also adapted to this condition. According to the size effects, different arm length is related to different wave motion. Different composite waves can be obtained in the output terminal by adjusting the arm length of the double quantum rings. Therefore, the structural characteristics of quantum rings will affect the transmission coefficient curves. Meanwhile, we can see that the Rashba spin-orbit interaction and the AB magnetic flux have effects on the shapes of the formants.

For a given quantum rings size and fixed Rashba parameters, the transmission coefficient as functions of the AB magnetic flux intensity for different φ_0 are shown in Fig. 5. The transmission coefficient shows periodic equal amplitude oscillation with increasing AB magnetic flux. Meanwhile, the curves for spin-up electrons are separated from the spin-down electrons. We can see that the area under the curves for the two kinds of spin state electrons become bigger as φ_0 changes, $\pi \to 2\pi/3 \to 3\pi/2 \to \pi/3$.

This implies that the average transmission coefficient increases with reducing angle φ_0. In other words, the hindrance to the tunneling electrons in the double quantum rings is reduced with decreasing angle φ_0. All of this will provide us with a theoretical guide to ringed spintronic device design.

4. Conclusions

In summary, based on the 1D quantum waveguide theory, we have studied the properties of the transmission coefficient in metal/semiconductor/metal double quantum rings connected in series considering the Rashba spin-orbit interaction and AB magnetic flux. We find that the transmission coefficient shows periodic amplitude oscillation with increasing semiconductor ring size. The average hindrance to the tunneling electrons in the unequal arm rings is stronger than that in equal ones. In addition, T^{σ} can be modified by changing the AB magnetic flux and the Rashba spin-orbit. When the total magnetic field is non-zero, we obtain $n_{\mathrm{x}} = \frac{N_{\mathrm{u}}}{N_{\mathrm{d}}} n_0$. The rule implies that the transmission coefficient is related to the two leads' relative position. Moreover, the transmission coefficient shows periodic equal amplitude oscillation with increasing external magnetic intensity. These features may be used to design a new spintronic device.

References

[1] Frustaglia D, Hentschel M, Richter K. Quantum transport in nonuniform magnetic fields: Aharonov-Bohm ring as a spin switch. Phys Rev Lett, 2001, 87: 256602

[2] Ionicioiu R, Amico I D. Mesoscopic Stern-Gerlach device to polarize spin currents. Phys Rev B, 2003, 67: 041307

[3] Frustaglia D, Richter K. Spin interference effects in ring conductors subject to Rashba coupling. Phys Rev B, 2004, 69: 235310

[4] Hentschel M, Schomerus H, Frustaglia D, et al. Aharonov-Bohm physics with spin I: geometric phases in one-dimensional ballistic rings. Phys Rev B, 2004, 69: 155326

[5] Shen S Q, Li Z J, Ma Z S. Controllable quantum spin precession by Aharonov-Chaser phase in a conducting ring. Appl Phys Lett, 2004, 84: 996

[6] Aeberhard U, Wakabayashi K, Sigrist M. Effect of spin-orbit coupling on the zero-conductance resonances in asymmetrically coupled one-dimensional rings. Phys Rev B, 2005, 72: 075382

[7] Berry M V. Quantal phase factors accompanying adiabatic changes. Proceedings of the Royal Society of London, Series A, 1984, 392: 45

[8] Loss D, Goldbart P, Balatsky A V. Berry's phase and persistent charge and spin currents in textured mesoscopic rings. Phys Rev Lett, 1990, 65: 1655

[9] Splettstoesser J, Governale M, Zulicke U. Persistent current in ballistic mesoscopic rings with Rashba spin-orbit coupling. Phys Rev B, 2003, 68: 165341

[10] Zhang Y T, Guo Y, Li Y C. Persistent spin currents in a quantum ring with multiple arms in the presence of spin-orbit interaction. Phys Rev B, 2005, 72: 125334

[11] Pletyukhov M, Gritsev V. Persistent currents in a multicomponent Tomonaga-Luttinger liquid: to a mesoscopic semiconductor ring with spin-orbit interaction. Phys Rev B, 2004, 70: 165316

[12] Wu H C, Guo Y, Chen X Y, et al. Giant persistent current in a quantum ring with multiple arms. Phys Rev B, 2003, 68: 125330

[13] Citro R, Romeo F, Marinaro M. Zero-conductance resonances and spin filtering effects in ring conductors subject to Rashba coupling. Phys Rev B, 2006, 74: 115329

[14] Meijer F E, Morpurgo A F, Klapwijk T M. One-dimensional ring in the presence of Rashba spin-orbit interaction: derivation of the correct Hamiltonian. Phys Rev B, 2002, 66: 033107

[15] Molnar B, Peeters F M, Vasilopoulos P. Spin-dependent magnetotransport through a ring due to spin-orbit interaction. Phys Rev B, 2004, 69: 155335